



HAL
open science

Structure, Morphology, and Surface Chemistry of Surgical Masks and Their Evolution up to 10 Washing Cycles

Louise Wittmann, Joseph Garnier, Naomi Sakata, Elisabeth Auzias, Martin Dumoulin, Nathanaël Barlier, Théotime Bergese, Lara Leclerc, Florence Grattard, Paul O Verhoeven, et al.

► To cite this version:

Louise Wittmann, Joseph Garnier, Naomi Sakata, Elisabeth Auzias, Martin Dumoulin, et al.. Structure, Morphology, and Surface Chemistry of Surgical Masks and Their Evolution up to 10 Washing Cycles. *ACS Applied Polymer Materials*, 2023, 5 (3), pp.2282-2288. 10.1021/acsapm.3c00145 . hal-04106860

HAL Id: hal-04106860

<https://hal.science/hal-04106860>

Submitted on 26 May 2023

HAL is a multi-disciplinary open access archive for the deposit and dissemination of scientific research documents, whether they are published or not. The documents may come from teaching and research institutions in France or abroad, or from public or private research centers.

L'archive ouverte pluridisciplinaire **HAL**, est destinée au dépôt et à la diffusion de documents scientifiques de niveau recherche, publiés ou non, émanant des établissements d'enseignement et de recherche français ou étrangers, des laboratoires publics ou privés.



Distributed under a Creative Commons Attribution 4.0 International License

Structure, Morphology, and Surface Chemistry of Surgical Masks and Their Evolution up to 10 Washing Cycles

Louise Wittmann, Joseph Garnier, Naomi Sakata, Elisabeth Auzias, Martin Dumoulin, Nathanaël Barlier, Théotime Bergese, Lara Leclerc, Florence Grattard, Paul O. Verhoeven, Jérémie Pourchez, Claude Botella, Jean-Marie Bluet, Béatrice Vacher, and José Penuelas*



Cite This: <https://doi.org/10.1021/acscapm.3c00145>



Read Online

ACCESS |



Metrics & More

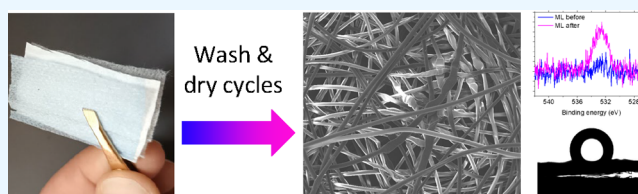


Article Recommendations



Supporting Information

ABSTRACT: The Covid-19 crisis has led to a massive surge in the use of surgical masks worldwide, causing risks of shortages and high pollution. Various decontamination techniques are currently being studied to reduce these risks by allowing the reuse of masks. In this study, surgical masks were washed up to 10 times, each cycle under the same conditions. The consequences of the washing cycles on the structure, fiber morphology, and surface chemistry have been studied through several characterization techniques: scanning electron microscopy, wetting angle measurements, infrared spectroscopy, X-ray diffraction, and X-ray photoelectrons spectroscopy. The washing process did not induce large changes in the hydrophobicity of the surface, the contact angle remaining constant throughout the cycles. The composition observed in the IR spectrum also remained unchanged for washed masks up to 10 cycles. Some slight variations were observed during X-ray analysis: the crystallinity of the fibers as well as the size of the crystals increases with the number of wash cycles. The XPS analysis shows that after 10 cycles, the surface of the masks underwent a slight oxidation. In the SEM images, changes were observed in the arrangement of the fibers, which are more visible the more times the mask has been washed: they align themselves in bundles, form areas with holes in the mask layer, and are crushed in some areas.



KEYWORDS: Covid-19, pandemic, surgical masks, decontamination, polypropylene, washing

INTRODUCTION

The Covid-19 crisis has had a significant impact on the entire world, including peoples, economies, or the environment since it began in March 2020.^{1–3} Airborne transmission is the dominant route of transmission of the SARS-CoV-2 virus,^{4,5} and this is why the widespread use of masks has considerably helped slow down the epidemic by reducing the flow of respiratory droplets emitted and inhaled.^{6–8} There are several types of masks, of varying effectiveness. In this study, we have chosen to study only type IIR surgical masks. Type IIR masks must have a bacterial filtration efficiency (BFE) greater than or equal to 98% and be splash-resistant (according to EN 14683+AC).

The massive use of masks has nevertheless generated massive pollution worldwide.^{9–11} Once in the oceans, these masks disintegrate into microparticles which significantly disrupt the local ecosystem.^{12,13} Moreover, the production of a single mask consumes about 10–30 Wh of energy and releases 59 g CO₂-eq greenhouse gas into the environment.¹⁴

Despite advances in the mask recycling process,^{15–17} mask decontamination is a promising way to address the above issues. Numerous decontamination methods have been tested in recent years, including UV irradiation,^{18–22} steam treatment,^{18,20,22–24} solvent treatment,^{18,20,22} dry heat treatment,^{18,20,22,23,25,26} and machine washing.^{27–31} Among these

methods, machine washing has the advantage of being easily accessible.

The studies on the decontamination of surgical masks by washing cycles have mainly focused on filtration efficiency³¹ and show that the efficiency of the mask is preserved after 10 washes. Several studies reported that exposure of polypropylene filters to aqueous or organic solvents can dissipate the electret charge and decrease the filtration efficiency,^{32,33} while Yim et al. do not report modification of the filtration efficiency.³⁴ However, these studies present few characterizations at the microscopic scale allowing the study of the mechanisms of mask degradation. Recent works have characterized the masks by a wide variety of techniques such as infrared spectroscopy,^{21,35} XRD,³⁶ and XPS.²¹ However, these techniques have not been used to see how surgical masks degrade after machine washing. In this context it is necessary to study their morphology, structure, and surface chemistry

Received: January 25, 2023

Accepted: February 13, 2023

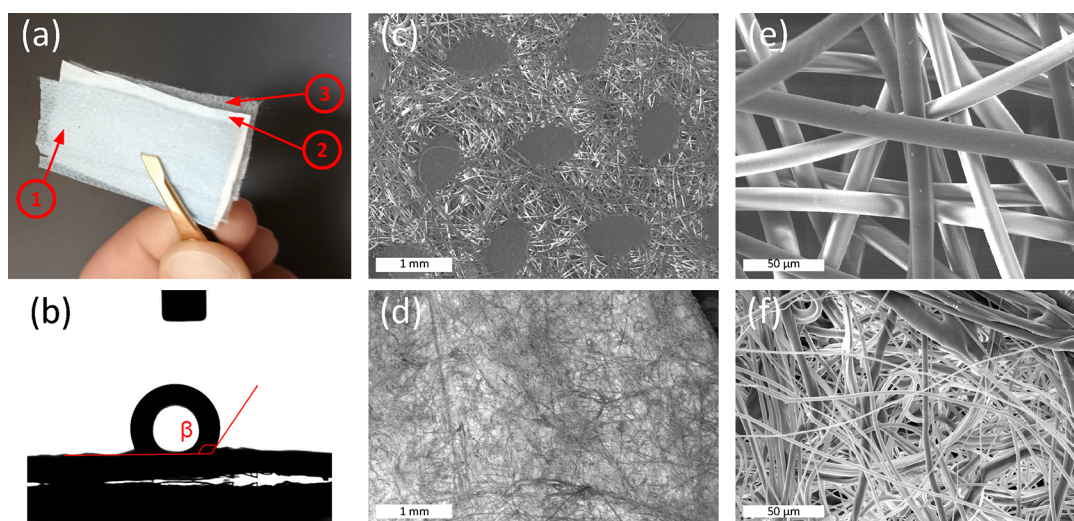


Figure 1. (a) Layers of facial mask: (1) outer layer (OL) (2) middle layer (ML) (3) inner layer (IL); (b) measurement of the wetting angle; (c) SEM view OL $\times 60$; (d) SEM view ML $\times 60$; (e) SEM view OL $\times 1200$; (f) SEM view ML $\times 1200$.

and their evolution during machine washing and drying cycles. In this study, masks were washed and dried up to 10 times. Their morphology, crystal structure, and surface chemistry were thoroughly characterized after different washing cycles, in order to identify possible degradation mechanisms of surgical masks.

■ STRUCTURE, SURFACE CHEMISTRY, AND MORPHOLOGY OF SURGICAL MASKS

The masks used in this study are M safe model 5055 masks, which are type IIR masks. To characterize the masks, SEM measurements, wetting angle measurements, IR spectrum, and X-ray analysis were performed on both the outer layer (OL) and middle layer (ML) of the masks.

Surgical masks are made of three layers (Figure 1(a)). The layers of the masks are made of nonwoven polypropylene (PP) fibers.³¹ The outer and inner layers of the masks exhibit no significant differences (except for their color), thus we chose to study the OL only out of the two. The ML is a filtering layer, made of meltblown polypropylene³⁷ that is charged during its manufacturing process, enabling a better filtration, the finest particles being captured by the charges at the surface of the mask.^{27,38,39}

Figure 1(b) shows a water droplet of 1 mL on the OL of the mask. β corresponds to the wetting angle of the droplet on this surface. Wetting angle measurements allow the determination of the hydrophobicity of the surfaces. The angle is formed at the interface between the air, the water, and the mask surface. For each sample, the wetting angle was measured 5 times, for more accurate results. For a mask without treatment, the average value is 133° with a standard deviation of 2° . These results are in agreement with that found in other articles.^{26,40} Only the OL was studied, as the ML is too hydrophobic for accurate wetting angle measurements.

Figure 1 panels (c, d, e, f) show SEM images of the OL (c, e) and ML (d, f) layers of an unwashed mask. The fibers of the OL have an average diameter of $30\ \mu\text{m}$, and are larger than the fibers of the ML, the average diameter of which is about $8\ \mu\text{m}$.⁴¹ On the OL, regular areas where the fibers are pressed together are visible, in order to maintain their structure and

arrangement. These areas are not present on the ML. These observations are consistent with those in the literature.^{21,26,40,42}

Figure 2 compares absorption spectra of ML and OL. Between $2950\ \text{cm}^{-1}$ and $2840\ \text{cm}^{-1}$, a large absorbance band is

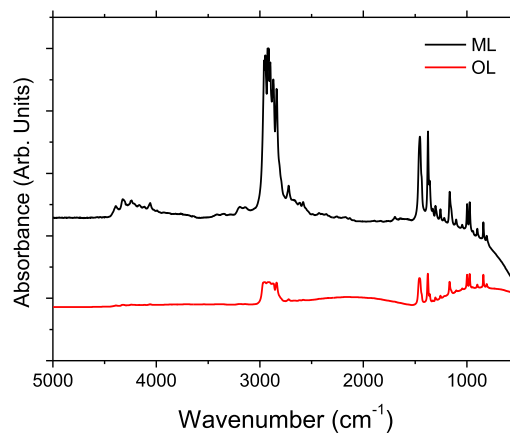


Figure 2. Comparison of absorbance spectrum of ML and OL.

visible. In this band, there are four observable peaks. The peaks at $2950\ \text{cm}^{-1}$ and around $1865\ \text{cm}^{-1}$ are the consequences of the elongations of the asymmetric and symmetric $-\text{CH}_3$. The peaks around $2920\ \text{cm}^{-1}$ and at $2840\ \text{cm}^{-1}$ characterize the asymmetric and symmetric $-\text{CH}_2$ stretching. The peaks observable at $1455\ \text{cm}^{-1}$ and $1375\ \text{cm}^{-1}$ correspond to the symmetric and asymmetric $-\text{CH}_3$ bending. The peak at $1165\ \text{cm}^{-1}$ characterizes $-\text{CH}_3$ wagging. The last 2 peaks at $997\ \text{cm}^{-1}$ and $971\ \text{cm}^{-1}$ are characteristic of the $-\text{CH}_3$ rocking. The OL and ML exhibit the same absorbance peaks with slight differences when comparing their relative intensities. The observed spectra are characteristic of PP.^{40,43,44}

X-ray diffraction (XRD) was used to characterize the phase composition and crystallinity of the masks. Both the OL and ML are semicrystalline and the major diffraction patterns are due to reflections from (110), (040), and (130) planes of the polypropylene, as observed in the form of peaks in Figure 3(a). The (110) plane is located at $2\theta = 14.1^\circ$, the (040) plane at 17.0° , and the (130) plane at 18.7° for both the OL and ML of

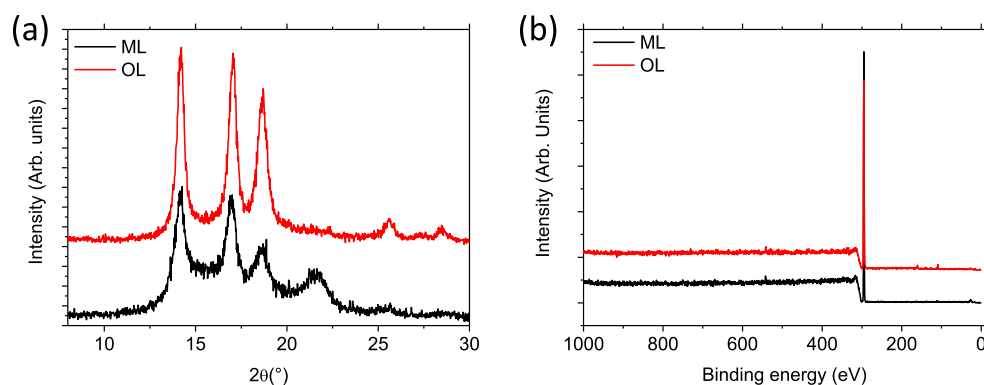


Figure 3. (a) XRD spectrum of ML and OL, unwashed mask, (b) XPS spectrum of ML and OL, unwashed mask.

the masks. These results correlate with the study of Larsen et al.⁴⁵ in which the same peaks were detected. Crystallinity was obtained with the following equation:

$$\text{ratio} = \frac{\text{crystalline area}}{\text{crystalline area} + \text{amorphous area}} \quad (1)$$

Crystallite size D was computed with the Sherrer's equation⁴⁶ with $K = 0.9$ for polypropylene:

$$D = K\lambda B \cos(\theta) \quad (2)$$

where λ is the source's wavelength and B is the full width at half-maximum. Using Fityk,⁴⁷ diffraction spectra fittings were conducted to obtain the mathematical parameters for each peak modeled by Gaussian curves (see [Supporting Information](#)). The useful parameters to calculate crystallinity and crystallite size were B and the area under the curve. From these fits we calculated a crystallinity of 55.9% for the OL and 42.1% for the ML. Similar results were found in a different study for a standard N95 mask, with a crystallinity of 46.5%.⁴⁵ The crystallinity of the ML is lower than that of the OL regardless of having washed the masks or not. The averaged crystal size calculated from (110), (040), and (130) peaks is 14.2 nm for OL and 12.0 nm for the ML. Our results correlate with the ones from Larsen et al. where the author found crystallinity ranging from 42 to 47% and crystal sizes ranging from 2.74 to 12.05 nm.⁴⁵

Figure 3(b) shows the XPS survey spectra of the OL and the ML. Both spectra exhibit a peak at 285.0 eV, which is exhibited in the presence of carbon C 1s as well as the presence of oxygen via the O 1s peak around 532.0 eV. The spectra and specifically the main peak is in agreement with C–C/C–H bonds. This is also consistent with the XRD diffraction measurements and the composition of polypropylene (PP).⁴⁸ There is no significant difference between the OL and ML, respectively, in black and red.

WASHING SURGICAL MASKS AND THEIR EVOLUTION

To measure the impact of wash and dry cycles, surgical masks were subjected to a number of wash cycles ranging from 0 to 10, with two masks for each number of washings. One cycle of washing consists of 40 min in a Miele Professional machine, at 40 °C, with 40 g of Ariel Powder Original detergent. The masks were then air-dried for 10 min, before a new cycle or characterizations. To perform the measurements, 1 cm² samples were cut from each mask, for each number of washes.

Figure 4 shows SEM images of the OL for different numbers of washing cycles highlighting the typical defects observed after

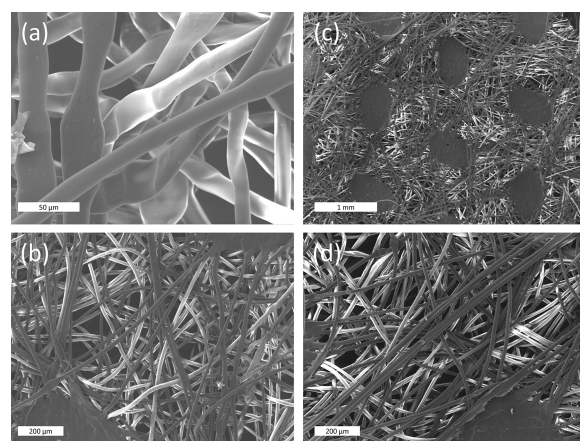


Figure 4. SEM view, OL (a) crushed fibers (8 washing cycles, ×1.2k); (b) holes in the structure of the fibers (8 washing cycles, ×220); (c) holes in the pressed areas (10 washing cycles, ×60) (d) Aligned fibers (10 washing cycles, ×220).

several washes. When increasing the number of washing cycles, some modifications became visible in comparison with the control mask (see SEM images of [Figure S5](#)). These defects include crushed fibers ([Figure 4\(a\)](#)), holes in the structure of the fibers ([Figure 4\(b\)](#)) or in the pressed areas ([4\(c\)](#)), and fiber alignment forming bundles ([Figure 4\(d\)](#)). The number of these defects increases with the number of wash cycles ([Figure S5](#)). The wash cycles seem to have an impact on the fibers and their distribution in the mask layer.

Wetting angles on the OL after 1, 3, 6, 8, and 10 washings were measured. For every wash, the wetting angle remained constant and stable. The wetting value is 133° with a standard deviation between 1° and 3°, each wetting angle corresponding to the average of 5 measurements. Washing cycles did not induce a significant impact on the hydrophobicity of the surface of the OL (see [Supporting Information](#)).

The evolution of chemical bonds was measured for masks after 1, 5, and 10 washes for both layers. After all wash cycles, the various absorbance peaks remained the same (see [Supporting Information](#)). The chemical bonds did not change due to washing cycles. The chemical composition of the PP is not altered by washing.

Regarding crystallinity, it increases with the number of washes for the OL of the mask ([Figure 5](#)). Crystallinity

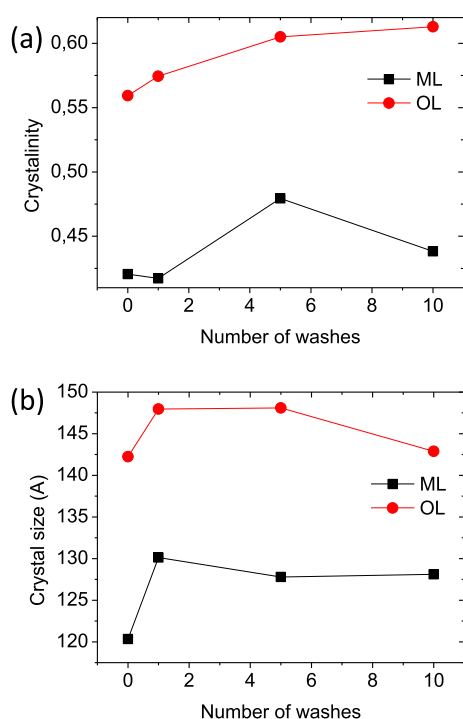


Figure 5. Crystallinity (a) and crystal size (b) of the ML (black) and OL (red) of the masks in polypropylene depending on the number of washes, obtained with XRD. In (b), each point represents the mean value of the values calculated in the three crystal planes (110), (040), and (130).

increases from 55.9% for the control mask (no wash) to 61.3% after washing the mask 10 times. In the ML, crystallinity fluctuates between 41.7% (1 cycle) and 47.9% (5 cycles). A slight increase between the control mask and after washing the mask 10 times (43.8%) is noted. Washing the mask seems to have an effect on crystallinity in both the OL and ML of the masks. Similar to crystallinity, crystallites are bigger in the OL than in the ML, regardless of the number of wash cycles. This result can be correlated with the SEM images (Figure 1) where the diameter of the polypropylene fibers in the OL are bigger than in the ML. In the ML, crystallite size increases with the number of washes between 120 and 130 Å. In the OL, crystallite size varies between 142 Å for the control mask (no wash) and 148 Å after 5 washes. There is a positive trend with 143 Å after 10 washes. Although the temperature used in the protocol was only 40 °C, its known mechanical stress can modify the crystallization temperature.⁴⁹

Figure 6 panels (a,b) show the C 1s core level of the OL and ML, respectively, measured before and after 10 wash and dry

cycles. We observe that the peak has broadened around 285.0 eV after washing, both on OL and ML. The broadening is the sign of a modification of the surface chemistry of the mask. In addition, there is an increase of intensity after 10 washes for the O 1s peak (Figure 6(c,d)), for both layers. It is likely that the water reacted with the polypropylene during washing and induced a slight oxidation of the polypropylene on the surface. This oxidation would also explain the broadening of the C 1s peak at 285 eV due to the presence of bonds between C and O. Such a broadening has been reported in ref 50 and was related to oxidation induced by a dry heating at 100 °C.

As shown in Figure 7, breathing resistance and bacterial filtration efficiency do not vary significantly depending on the number of washing cycle. On the one hand, no significant impact of washing on bacterial filtration efficiency was observed. We can notice that the mask is of excellent filtration quality with an efficiency very closed to 100%. On the other hand, the level of breathing resistance remains globally constant around 45 Pa cm² and indicates that it is a type IIR mask (mask showing a breathing resistance lower than 60 Pa cm²), and not type II mask (mask showing a breathing resistance lower than 40 Pa cm²) according to the requirement of EN 14683+AC (2019) standard.

CONCLUSION

This study shows that 10 wash and dry cycles do not induce major changes in the physicochemical structure of a type IIR mask. The only chemical change observed is a slight oxidation on the surface. The surface tension and chemical bonds remain unchanged. The physical structure is slightly degraded on the OL with the formation of holes, areas with less fibers, or crushed fibers. Studies conducted by Alcaraz et al.³¹ led to the conclusion that type IIR masks can be washed and reused up to 10 times which is in agreement with our results. Machine washing appears to be a promising solution for mask decontamination and reuse.

EXPERIMENTAL SECTION

The washing method is one of the simplest decontamination methods. The machine used for this protocol is a model found in laundromats for the general public. The rotation speed of the washing machine was 1200 rpm. Only surgical masks are washed in every cycle to avoid degradations due to other textiles that are difficult to quantify. The detergent used here is Ariel Powder Original. It is effective at 40 °C, corresponding to the water temperature for this protocol. The particularity of a powder detergent is that it contains oxygenated bleaching agents (15%). Due to oxido-reduction reactions, these detergents are more aggressive on textiles. It is expected that oxido-reduction reactions may affect the filter. Between each washing cycle, the masks are air-dried for 10 min.

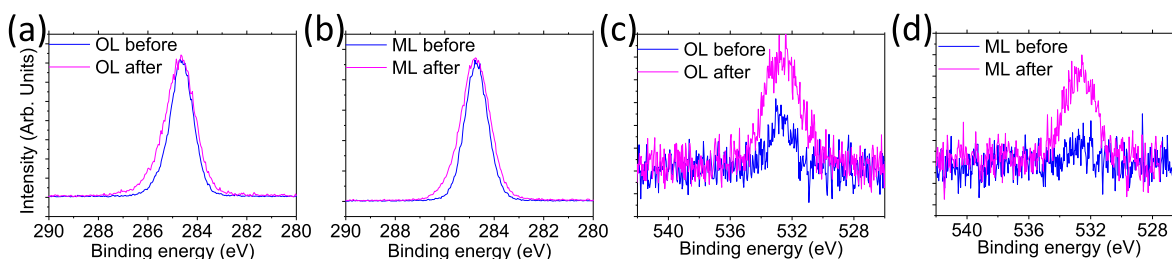


Figure 6. C 1s core level measured before and after 10 cycles of washes for the OL (a) and the ML (b). O 1s core level measured before and after 10 cycles of washes for the OL (c) and the ML (d).

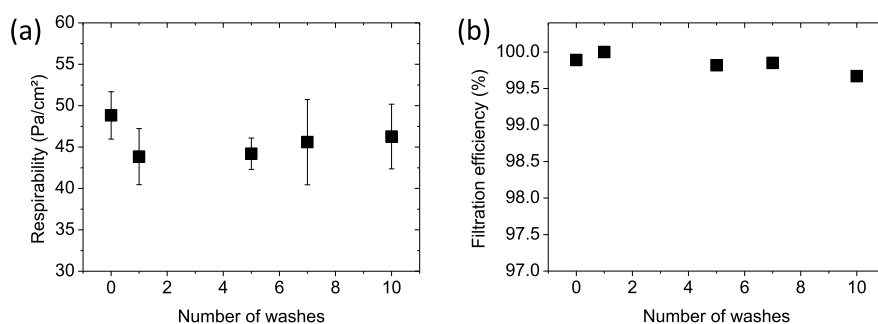


Figure 7. Respirability (a) and filtration efficiency (b) of the surgical mask as a function of the number of washes.

The SEM images were taken with a TESCAN MIRA3 microscope. Small squares of masks were cut (around 0.25 cm^2) in each layer. The samples were placed on double-sided sticky carbon pads, which were stuck to an aluminum plane. The samples were then gold-coated by a sputtering device. The images were taken with an accelerating voltage of 10 kV. The wetting angle measurements were carried out with a tensiometer. The droplet had a constant volume of 1 L. The measurements were repeated five times for each layer. Infrared measurements were performed in a standard configuration for the midinfrared range (KBr beamsplitter, pyroelectric DTGS detector) using a Bruker vertex 70 spectrometer. XPS measurements were carried out in a Prevac spectrometer equipped with a focused monochromatic X-ray source Al K (1486.6 eV), in a base pressure less than 109 mbar. The different spectra were recorded at 45° exit angle. The energy calibration was checked with a gold reference ($\text{Au } 4f$ at $84(\pm 0.1) \text{ eV}$) just before the experiment. XRD measurements were performed with a diffractometer equipped with a rotating anode operating at 9 kW monochromatized with a two reflection Ge (400) crystal which selects the Cu K 1 radiation (wavelength = 1.5406 \AA). The detector was a scintillation counter.

Breathing resistance was evaluated according to the EN 14683+AC (2019) standard procedure for medical face masks as previously described.^{51,52} Briefly, the breathing resistance was calculated by measuring the differential pressure drop across the mask material. The mask was attached between two sample holders with a circular cross-section of 4.9 cm^2 (25 mm diameter), and the air passed through the mask at a fixed airflow rate of 8 L min^{-1} . The differential pressure or breathing resistance was expressed in Pa cm^2 . The value is the average of five measurements of the mask sample.

The evaluation of the bacterial filtration efficiency was performed according to the EN 14683:2019 standard for the performance of medical masks and using a previously published experimental procedure.^{52,53} Briefly, an aerosol stream containing a known charge of *Staphylococcus aureus* ATCC 29213 is generated using an E-flow mesh nebulizer (Pari GmbH, Starnberg, Germany). The generated aerosol is then drawn through a aerosol chamber at a constant flow of 28.3 L min^{-1} by a vacuum pump. The mask samples are clamped between the aerosol chamber and a six stage viable Andersen Cascade Impactor (Tisch Environmental) where 90 mm plastic Petri dishes, containing an agar culture medium, are used as impaction plates. Depending on the orifice diameters, droplets of a given class-size impact on the Petri dish and trigger the formation of a colony of bacteria (expressed in Colony Forming Units or CFU). The Petri dishes were incubated at $37 \pm 2 \text{ }^\circ\text{C}$ for $22 \pm 2 \text{ h}$. The CFU are counted with an automatic colony counter (Scan 4000, Interscience), and the bacterial filtration efficiency (expressed in %) is calculated owing to positive and negative controls.

■ ASSOCIATED CONTENT

SI Supporting Information

The Supporting Information is available free of charge at <https://pubs.acs.org/doi/10.1021/acsapm.3c00145>.

Wetting angle measurements as a function of the number of washes; evolution of the absorbance for the

outer and middle layer as a function of the number of washes; X-ray diffraction fitting; supplementary SEM images for 1, 6, and 10 washes (PDF)

■ AUTHOR INFORMATION

Corresponding Author

José Penuelas – Univ Lyon, Ecole Centrale de Lyon, CNRS, INSA Lyon, Université Claude Bernard Lyon 1, 69130 Ecully, France; orcid.org/0000-0002-5635-7346; Email: jose.penuelas@ec-lyon.fr

Authors

Louise Wittmann – Univ Lyon, Ecole Centrale de Lyon, CNRS, INSA Lyon, Université Claude Bernard Lyon 1, 69130 Ecully, France

Joseph Garnier – Univ Lyon, Ecole Centrale de Lyon, CNRS, INSA Lyon, Université Claude Bernard Lyon 1, 69130 Ecully, France

Naomi Sakata – Univ Lyon, Ecole Centrale de Lyon, CNRS, INSA Lyon, Université Claude Bernard Lyon 1, 69130 Ecully, France

Elisabeth Auzias – Univ Lyon, Ecole Centrale de Lyon, CNRS, INSA Lyon, Université Claude Bernard Lyon 1, 69130 Ecully, France

Martin Dumoulin – Univ Lyon, Ecole Centrale de Lyon, CNRS, INSA Lyon, Université Claude Bernard Lyon 1, 69130 Ecully, France

Nathanaël Barlier – Univ Lyon, Ecole Centrale de Lyon, CNRS, INSA Lyon, Université Claude Bernard Lyon 1, 69130 Ecully, France

Théotime Bergese – Univ Lyon, Ecole Centrale de Lyon, CNRS, INSA Lyon, Université Claude Bernard Lyon 1, 69130 Ecully, France

Lara Leclerc – Mines Saint-Etienne, Université Jean Monnet Saint-Etienne, INSERM, F-42023 Saint-Etienne, France

Florence Grattard – CIRI, Centre International de Recherche en Infectiologie, GIMAP team, Université de Lyon, Inserm, U1111, CNRS, UMR5308, ENS Lyon, Université Claude Bernard Lyon 1, 69364 Lyon, France; Faculty of Medicine, Université Jean Monnet St-Etienne, 42000 St-Etienne, France; Department of Infectious Agents and Hygiene, University Hospital of St-Etienne, 42000 St-Etienne, France

Paul O. Verhoeven – CIRI, Centre International de Recherche en Infectiologie, GIMAP team, Université de Lyon, Inserm, U1111, CNRS, UMR5308, ENS Lyon, Université Claude Bernard Lyon 1, 69364 Lyon, France; Faculty of Medicine, Université Jean Monnet St-Etienne, 42000 St-Etienne, France; Department of Infectious Agents and Hygiene, University

Hospital of St-Etienne, 42000 St-Etienne, France;

orcid.org/0000-0003-4352-1263

Jérémie Pourchez – Mines Saint-Etienne, Université Jean Monnet Saint-Etienne, INSERM, F-42023 Saint-Etienne, France

Claude Botella – Univ Lyon, Ecole Centrale de Lyon, CNRS, INSA Lyon, Université Claude Bernard Lyon 1, 69130 Ecully, France

Jean-Marie Bluet – Univ Lyon, Ecole Centrale de Lyon, CNRS, INSA Lyon, Université Claude Bernard Lyon 1, 69130 Ecully, France

Béatrice Vacher – Université de Lyon, 69134 Ecully, France

Complete contact information is available at:

<https://pubs.acs.org/10.1021/acsapm.3c00145>

Notes

The authors declare no competing financial interest.

ACKNOWLEDGMENTS

The authors thank the NanoLyon platform for access to the equipment. Thomas Gehin is acknowledged for technical assistance.

REFERENCES

- (1) Xiong, J.; Lipsitz, O.; Nasri, F.; Lui, L. M.W.; Gill, H.; Phan, L.; Chen-Li, D.; Jacobucci, M.; Ho, R.; Majeed, A.; McIntyre, R. S. Impact of COVID-19 pandemic on mental health in the general population: A systematic review. *Journal of affective disorders* **2020**, *277*, 55–64.
- (2) Ozili, P. K.; Arun, T. Spillover of COVID-19: impact on the Global Economy. *Managing Inflation and Supply Chain Disruptions in the Global Economy*; IGI Global **2022**, 41–61.
- (3) Bashir, M. F.; MA, B.; Shahzad, L. A brief review of socio-economic and environmental impact of Covid-19. *Air Quality, Atmosphere & Health* **2020**, *13*, 1403–1409.
- (4) Rabaan, A. A. Airborne transmission of SARS-CoV-2 is the dominant route of transmission: droplets and aerosols. *Le Infezioni in Medicina* **2021**, *29*, 10–19.
- (5) Klompas, M.; Baker, M. A.; Rhee, C. Airborne transmission of SARS-CoV-2: theoretical considerations and available evidence. *Jama* **2020**, *324*, 441–442.
- (6) Cheng, Y.; Ma, N.; Witt, C.; Rapp, S.; Wild, P. S.; Andreae, M. O.; Poschl, U.; Su, H. Face masks effectively limit the probability of SARS-CoV-2 transmission. *Science* **2021**, *372*, 1439–1443.
- (7) O'Dowd, K.; Nair, K. M.; Forouzandeh, P.; Mathew, S.; Grant, J.; Moran, R.; Bartlett, J.; Bird, J.; Pillai, S. C. Face masks and respirators in the fight against the COVID-19 pandemic: A review of current materials, advances and future perspectives. *Materials* **2020**, *13*, 3363.
- (8) Chu, D. K.; Akl, E. A.; Duda, S.; Solo, K.; Yaacoub, S.; Schunemann, H. J.; Chu, D. K.; Akl, E. A.; El-harakeh, A.; Bognanni, A.; Lotfi, T.; Loeb, M.; Hajizadeh, A.; Bak, A.; Izcovich, A.; Cuello-Garcia, C. A.; Chen, C.; Harris, D. J.; Borowiack, E.; Chamseddine, F.; Schunemann, F.; Morgano, G. P.; Muti Schunemann, G. E. U.; Chen, G.; Zhao, H.; Neumann, I.; Chan, J.; Khabsa, J.; Hneiny, L.; Harrison, L.; Smith, M.; Rizk, N.; Giorgi Rossi, P.; AbiHanna, P.; El-khoury, R.; Stalteri, R.; Baldeh, T.; Piggott, T.; Zhang, Y.; Saad, Z.; Khamis, A.; Reinap, M.; Duda, S.; Solo, K.; Yaacoub, S.; Schunemann, H. J. Physical distancing, face masks, and eye protection to prevent person-to-person transmission of SARS-CoV-2 and COVID-19: a systematic review and meta-analysis. *lancet* **2020**, *395*, 1973–1987.
- (9) Aragaw, T. A. Surgical Face Masks as a Potential Source for Microplastic Pollution in the COVID-19 Scenario. *Mar. Pollut. Bull.* **2020**, *159*, 111517.
- (10) Roberts, K. P. Coronavirus face masks: an environmental disaster that might last generations. *The Conversation* **2020**.
- (11) Dybas, C. L. Surgical masks on the beach: COVID-19 and marine plastic pollution. *Oceanography* **2021**, *34*, 105.
- (12) Pizarro-Ortega, C. I.; Dioses-Salinas, D. C.; Fernandez Severini, M. D.; Forero Lopez, A. D.; Rimondino, G. N.; Benson, N. U.; Dobaradaran, S.; De-la-Torre, G. E. Degradation of Plastics Associated with the COVID-19 Pandemic. *Mar. Pollut. Bull.* **2022**, *176*, 113474.
- (13) Selvaranjan, K.; Navaratnam, S.; Rajeev, P.; Ravintherakumar, N. Environmental Challenges Induced by Extensive Use of Face Masks during COVID-19: A Review and Potential Solutions. *Environmental Challenges* **2021**, *3*, 100039.
- (14) Klemes, J. J.; Fan, Y. V.; Jiang, P. The Energy and Environmental Footprints of COVID-19 Fighting Measures - PPE, Disinfection, Supply Chains. *Energy* **2020**, *211*, 118701.
- (15) Asim, N.; Badiei, M.; Sopian, K. Review of the Valorization Options for the Proper Disposal of Face Masks during the COVID-19 Pandemic. *Environmental Technology & Innovation* **2021**, *23*, 101797.
- (16) Kilmartin-Lynch, S.; Saberian, M.; Li, J.; Roychand, R.; Zhang, G. Preliminary Evaluation of the Feasibility of Using Polypropylene Fibres from COVID-19 Single-Use Face Masks to Improve the Mechanical Properties of Concrete. *Journal of Cleaner Production* **2021**, *296*, 126460.
- (17) Maderuelo-Sanz, R.; Acedo-Fuentes, P.; Garcia-Cobos, F. J.; Sanchez-Delgado, F. J.; Mota-Lopez, M. I.; Meneses-Rodriguez, J. M. The Recycling of Surgical Face Masks as Sound Porous Absorbers: Preliminary Evaluation. *Science of The Total Environment* **2021**, *786*, 147461.
- (18) Ou, Q.; Pei, C.; Chan Kim, S.; Abell, E.; Pui, D. Y.H. Evaluation of Decontamination Methods for Commercial and Alternative Respirator and Mask Materials – View from Filtration Aspect. *J. Aerosol Sci.* **2020**, *150*, 105609.
- (19) Center for Devices Health and Radiological. *UV Lights and Lamps: Ultraviolet-C Radiation, Disinfection, and Coronavirus*; USFDA, 2021. <https://www.fda.gov/medical-devices/coronavirus-covid-19-and-medical-devices/uv-lights-and-lamps-ultraviolet-c-radiation-disinfection-and-coronavirus>.
- (20) Suen, C. Y.; Leung, H. H.; Lam, K. W.; Hung, K. P. S.; Chan, M. Y.; Kwan, J. K. C. Feasibility of Reusing Surgical Mask Under Different Disinfection Treatments. *MedRxiv* **2020**, 16.20102178.
- (21) Kumar, S.; Karmacharya, M.; Joshi, S. R.; Gulenko, O.; Park, J.; Kim, G.-H.; Cho, Y.-K. Photoactive Antiviral Face Mask with Self-Sterilization and Reusability. *Nano Lett.* **2021**, *21*, 337–343.
- (22) Cortes, M. F.; Espinoza, E. P. S.; Noguera, S. L. V.; Silva, A. A.; de Medeiros, M. E. S. A.; Villas Boas, L. S.; Ferreira, N. E.; Tozetto-Mendoza, T. R.; Morais, F. G.; de Queiroz, R. S.; de Proenca, A. C. T.; Guimaraes, T.; Guedes, A. R.; Letaif, L. S. H.; Montal, A. C.; Mendes-Correa, M. C.; John, V. M.; Levin, A. S.; Costa, S. F. Decontamination and Re-Use of Surgical Masks and Respirators during the COVID-19 Pandemic. *International Journal of Infectious Diseases* **2021**, *104*, 320–28.
- (23) Li, D. F.; Cadnum, J. L.; Redmond, S. N.; Jones, L. D.; Donskey, C. J. It's Not the Heat, It's the Humidity: Effectiveness of a Rice Cooker-Steamer for Decontamination of Cloth and Surgical Face Masks and N95 Respirators. *American Journal of Infection Control* **2020**, *48*, 854–55.
- (24) Li, D. F.; Cadnum, J. L.; Redmond, S. N.; Jones, L. D.; Pearlmutter, B.; Haq, M. F.; Donskey, C. J. Steam Treatment for Rapid Decontamination of N95 Respirators and Medical Face Masks. *American Journal of Infection Control* **2020**, *48*, 855–57.
- (25) Xiang, Y.; Song, Q.; Gu, W. Decontamination of Surgical Face Masks and N95 Respirators by Dry Heat Pasteurization for One Hour at 70°C. *American Journal of Infection Control* **2020**, *48*, 880–82.
- (26) Sales, E.; Mulatier, N.; Wittmann, L.; Fernandes, A.; Vacher, B.; Penuelas, J. Effect of dry heat treatment between room temperature and 160 °C on surgical masks. *Mater. Lett.* **2022**, *308*, 131270.
- (27) Hossain, E.; Bhadra, S.; Jain, H.; Das, S.; Bhattacharya, A.; Ghosh, S.; Levine, D. Recharging and Rejuvenation of Decontaminated N95 Masks. *Phys. Fluids* **2020**, *32*, 93304.

- (28) Wang, D.; Sun, B.-C.; Wang, J.-X.; Zhou, Y.-Y.; Chen, Z.-W.; Fang, Y.; Yue, W.-H.; Liu, S.-M.; Liu, K.-Y.; Zeng, X.-F.; Chu, G.-W.; Chen, J.-F. Can Masks Be Reused After Hot Water Decontamination During the COVID-19 Pandemic. *Engineering* **2020**, *6*, 1115–21.
- (29) Mackenzie, D. Reuse of N95 Masks. *Engineering* **2020**, *6*, 593–96.
- (30) Charvet, A.; Bardin-Monnier, N.; Thomas, D.; Dufaud, O.; Pfrimmer, M.; Barrault, M.; Bourrous, S.; Mocho, V.; Ouf, F.-X.; Poirier, S.; Jeanmichel, L.; Segovia, C.; Ferry, D.; Grauby, O. Impact of Washing Cycles on the Performances of Face Masks. *J. Aerosol Sci.* **2020**, *160*, 105914.
- (31) Alcaraz, J.-P.; Le Coq, L.; Pourchez, J.; Thomas, D.; Chazelet, S.; Boudry, L.; Barbado, M.; Silvent, S.; Dessale, C.; Antoine, F.; Guimier-Pingault, C.; Cortella, L.; Rouif, S.; Bardin-Monnier, N.; Charvet, A.; Dufaud, O.; Leclerc, L.; Montigaud, Y.; Laurent, C.; Verhoeven, P.; Joubert, A.; Bouhanguel, A.; Andres, Y.; Gaffe, J.; Martin, D. K.; Huet, C.; Boisset, S.; Maurin, M.; Rumeau, P.; Charlot, F.; Richaud, E.; Moreau-Gaudry, A.; Bonnetterre, V.; Cinquin, P.; Landelle, C. Reuse of Medical Face Masks in Domestic and Community Settings without Sacrificing Safety: Ecological and Economical Lessons from the Covid-19 Pandemic. *Chemosphere* **2022**, *288*, 132364.
- (32) Liao, L.; Xiao, W.; Zhao, M.; Yu, X.; Wang, H.; Wang, Q.; Chu, S.; Cui, Y. Can N95 respirators be reused after disinfection? How many times? *ACS Nano* **2020**, *14*, 6348–6356.
- (33) Sorci, M.; Fink, T. D.; Sharma, V.; Singh, S.; Chen, R.; Arduini, B. L.; Dovidenko, K.; Heldt, C. L.; Palermo, E. F.; Zha, R. H. Virucidal N95 Respirator Face Masks via Ultrathin Surface-Grafted Quaternary Ammonium Polymer Coatings. *ACS Appl. Mater. Interfaces* **2022**, *14*, 25135.
- (34) Yim, W.; Cheng, D.; Patel, S. H.; Kou, R.; Meng, Y. S.; Jokerst, J. V. KN95 and N95 respirators retain filtration efficiency despite a loss of dipole charge during decontamination. *ACS Appl. Mater. Interfaces* **2020**, *12*, 54473–54480.
- (35) Jiang, Z.; Hu, M.; Fan, L.; Pan, Y.; Tang, W.; Zhai, G.; Lu, Y. Combining Visible Light and Infrared Imaging for Efficient Detection of Respiratory Infections such as COVID-19 on Portable Device. *ArXiv* **2020**, 2004.06912.
- (36) Zhang, H.; Liu, N.; Zeng, Q.; Liu, J.; Zhang, X.; Ge, M.; Zhang, W.; Li, S.; Fu, Y.; Zhang, Y. Design of Polypropylene Electret Melt Blown Nonwovens with Superior Filtration Efficiency Stability through Thermally Stimulated Charging. *Polymers* **2020**, *12*, 2341.
- (37) Chua, M. H.; Cheng, W.; Goh, S. S.; Kong, J.; Li, B.; Lim, J. Y. C.; Mao, L.; Wang, S.; Xue, K.; Yang, L.; Ye, E.; Zhang, K.; Cheong, W. C. D.; Tan, B. H.; Li, Z.; Tan, B. H.; Loh, X. J. Face Masks in the New COVID-19 Normal: Materials, Testing, and Perspectives. *Research* **2020**, *2020*, 7286735.
- (38) Tcharkhtchi, A.; Abbasnezhad, N.; Zarbini Seydani, M.; Zirak, N.; Farzaneh, S.; Shirinbayan, M. An Overview of Filtration Efficiency through the Masks: Mechanisms of the Aerosols Penetration. *Bioactive Materials* **2021**, *6*, 106–22.
- (39) Sankhyan, S.; Heinselman, K. N.; Ciesielski, P. N.; Barnes, T.; Himmel, M. E.; Teed, H.; Patel, S.; Vance, M. E. Filtration Performance of Layering Masks and Face Coverings and the Reusability of Cotton Masks after Repeated Washing and Drying. *Aerosol and Air Quality Research* **2021**, *21*, 210117.
- (40) Ullah, S.; Ullah, A.; Lee, J.; Jeong, Y.; Hashmi, M.; Zhu, C.; Joo, K. I.; Cha, H. J.; Kim, I. S. Reusability Comparison of Melt-Blown vs Nanofiber Face Mask Filters for Use in the Coronavirus Pandemic. *ACS Applied Nano Materials* **2020**, *3*, 7231–41.
- (41) Peebles, L. Face Masks: What the Data Say. *Nature* **2020**, *586*, 186–89.
- (42) Liao, L.; Xiao, W.; Zhao, M.; Yu, X.; Wang, H.; Wang, Q.; Chu, S.; Cui, Y. Can N95 Respirators Be Reused after Disinfection? How Many Times? *ACS Nano* **2020**, *14*, 6348–6356.
- (43) Szefer, E. M.; Majka, T. M.; Pielichowski, K. Characterization and Combustion Behavior of Single-Use Masks Used during COVID-19 Pandemic. *Materials* **2021**, *14*, 3501.
- (44) Crespo, C.; Ibarz, G.; Saenz, C.; Gonzalez, P.; Roche, S. Study of Recycling Potential of FFP2 Face Masks and Characterization of the Plastic Mix-Material Obtained. A Way of Reducing Waste in Times of Covid-19. *Waste and Biomass Valorization* **2021**, *12*, 6423–6432.
- (45) Larsen, G. S.; Cheng, Y.; Daemen, L. L.; Lamichhane, T. N.; Hensley, D. K.; Hong, K.; Meyer, H. M.; Monaco, S. J.; Levine, A. M.; Lee, R. J.; Betters, E.; Sitzlar, K.; Heineman, J.; West, J.; Lloyd, P.; Kunc, V.; Love, L.; Theodore, M.; Paranthaman, M. P. Polymer, Additives, and Processing Effects on N95 Filter Performance. *ACS Applied Polymer Materials* **2021**, *3*, 1022–1031.
- (46) Xiao, H.; Gui, J.; Chen, G.; Xiao, C. Study on correlation of filtration performance and charge behavior and crystalline structure for melt-blown polypropylene electret fabrics. *J. Appl. Polym. Sci.* **2015**, *132*, 42807.
- (47) Wojdyr, M. Fityk: a general-purpose peak fitting program. *J. Appl. Crystallogr.* **2010**, *43*, 1126–1128.
- (48) Hantsche, H. High resolution XPS of organic polymers, the scienta ESCA300 database. By G. Beamson and D. Briggs, Wiley, Chichester 1992, 295 pp., hardcover, £ 65.00, ISBN 0–471–93592–1. *Adv. Mater.* **1993**, *5*, 778–778.
- (49) Sowinski, P.; Veluri, S.; Piorkowska, E. Crystallization of Isotactic Polypropylene Nanocomposites with Fibrillated Poly (tetrafluoroethylene) under Elevated Pressure. *Polymers* **2022**, *14*, 88.
- (50) Yan, S.; Stackhouse, C. A.; Waluyo, I.; Hunt, A.; Kisslinger, K.; Head, A. R.; Bock, D. C.; Takeuchi, E. S.; Takeuchi, K. J.; Wang, L.; Marschilok, A. C. Reusing Face Covering Masks: Probing the Impact of Heat Treatment. *ACS Sustainable Chem. Eng.* **2021**, *9*, 13545–13558.
- (51) Whyte, H. E.; Joubert, A.; Leclerc, L.; Sarry, G.; Verhoeven, P.; Le Coq, L.; Pourchez, J. Reusability of face masks: Influence of washing and comparison of performance between medical face masks and community face masks. *Environmental Technology & Innovation* **2022**, *28*, 102710.
- (52) Whyte, H. E.; Joubert, A.; Leclerc, L.; Sarry, G.; Verhoeven, P.; Le Coq, L.; Pourchez, J. Impact of washing parameters on bacterial filtration efficiency and breathability of community and medical facemasks. *Sci. Rep.* **2022**, *12*, 1–11.
- (53) Whyte, H. E.; Montigaud, Y.; Audoux, E.; Verhoeven, P.; Prier, A.; Leclerc, L.; Sarry, G.; Laurent, C.; Le Coq, L.; Joubert, A.; Pourchez, J. Comparison of bacterial filtration efficiency vs. particle filtration efficiency to assess the performance of non-medical face masks. *Sci. Rep.* **2022**, *12*, 1–8.